RKKY interaction of magnetic impurities in Dirac and Weyl semimetals

Hao-Ran Chang, Jianhui Zhou, Shi-Xiong Wang, Wen-Yu Shan, and Di Xiao

Phys. Rev. B **92**, 241103 — Published 3 December 2015

DOI: 10.1103/PhysRevB.92.241103

RKKY Interaction of Magnetic Impurities in Dirac and Weyl Semimetals

Hao-Ran Chang,[1] Jianhui Zhou,[2,*] Shi-Xiong Wang,[1] Wen-Yu Shan,[2] and Di Xiao[2,†]

[1] *Department of Physics and Institute of Solid State Physics, Sichuan Normal University, Chengdu, Sichuan 610066, China*

[2] *Department of Physics, Carnegie Mellon University, Pittsburgh, Pennsylvania 15213, USA*

We theoretically study the Ruderman-Kittel-Kasuya-Yosida (RKKY) interaction between magnetic impurities in both Dirac and Weyl Semimetals (SMs). We find that the internode process, as well as the unique three dimensional spin-momentum locking, has significant influences on the RKKY interaction, resulting in both a Heisenberg and an Ising term, and an additional Dzyaloshinsky-Moriya term if the inversion symmetry is absent. These interactions can lead to rich spin textures and possible ferromagnetism in Dirac and time reversal symmetry-invariant Weyl SMs. The effect of anisotropic Dirac and Weyl nodes on the RKKY interaction is also discussed. Our results provide an alternative scheme to engineer topological SMs and shed new light on the application of Dirac and Weyl SMs in spintronics.

PACS numbers: 71.55.Ak, 03.65.Vf, 75.30.Hx

Three dimensional (3D) Dirac semimetals (SMs) [1] are topological states of matter and can be seen as bulk analogue of graphene. Their conduction and valence bands with linear dispersion touch each other at a finite number of points, called the Dirac nodes, in the 3D Brillouin zone. Dirac nodes are four-fold degenerate, protected by both time reversal symmetry (TRS) and inversion symmetry. Breaking either symmetry in Dirac SMs leads to Weyl SMs [2], which host Weyl nodes. These Weyl nodes can be viewed as effective magnetic monopoles in the momentum space [3], acting as the source and drain of the Berry curvature field [4]. This nontrivial topology can lead to exotic superfluid [5] and superconducting phases [6], unique Fermi arc state [7], helical spin order [8], various novel electromagnetic responses, such as the chiral anomaly [9, 10], the chiral magnetic effect [11], negative magnetoresistance [12], and the chiral Hall effect [13].

Many aforementioned exotic phenomena rely on the separation of Weyl nodes in momentum space due to the intrinsic TRS breaking. So far, angle-resolved photoemission spectroscopy and magnetotransport measurements have identified $(Bi_{1-x}In_x)_2Se_3$ [14], Na_3Bi [15], and Cd_3As_2 [16] as Dirac SMs, and noncentrosymmetric transition metal monosphides TaAs, NbAs, NbP and TaP as Weyl SMs [17–22]. There are, however, few experimental realizations of TRS breaking Weyl SMs without Landau quantization [23]. Even though a magnetic field can break the TRS, it inevitably couples to both the spin and orbital motion of electrons through Zeeman splitting and Landau quantization, respectively. On the other hand, magnetic doping technique has recently been utilized in experimental implementation of the quantum anomalous Hall effect in thin films of topological insulators [24]. Thus, one may naturally wonder whether Weyl SMs without TRS can emerge from Dirac and time reversal invariant Weyl SMs through introducing magnetic dopants rather than applying a magnetic field.

Motivated by the above observation, in this paper we study the Ruderman-Kittel-Kasuya-Yosida (RKKY) interaction between magnetic dopants in both Dirac and Weyl SMs. We find that the internode process, as well as the unique 3D spin-momentum locking, has significant influences on the RKKY interaction, resulting in both a Heisenberg and an Ising term, and an additional Dzyaloshinsky-Moriya term if the inversion symmetry is absent. These interactions can lead to rich spin textures and possibly ferromagnetism in Dirac and TRS-invariant Weyl SMs. The effect of anisotropic Dirac and Weyl nodes on the RKKY interaction is also discussed. Our results provide an alternative scheme to engineer topological SMs and shed new light on the application of Dirac and Weyl SMs in spintronics.

In general, a pair of Weyl nodes of opposite chirality can be described by the following Hamiltonian

$$H_0 = \chi\big(v_F\boldsymbol{\sigma}\cdot(\boldsymbol{k}-\chi\boldsymbol{Q})+\sigma_0 Q_0\big)\,, \tag{1}$$

where $\boldsymbol{k}$ is the wave vector, v_F is the Fermi velocity, and $\chi = \pm 1$ refers to the chirality of the Weyl nodes. If $(\boldsymbol{Q}, Q_0) = 0$, the two Weyl nodes overlap with each other and the Hamiltonian H_0 describes Dirac SMs (see Fig. 1(a)). For noncentrosymmetric Weyl SMs that preserve the TRS, $\boldsymbol{Q}$ must be zero and Q_0 can be nonzero. As a result, the two Weyl nodes are located at the same $\boldsymbol{k}$-point but can have different energies as shown in Fig. 1(b). Hence for a given carrier density, there are two unequal Fermi wave vectors. On the other hand, for Weyl SMs with broken TRS but with inversion symmetry, we have $Q_0 = 0$ and $\boldsymbol{Q} \neq 0$; the two Weyl modes have the same energy but reside at different $\boldsymbol{k}$-points $\pm\boldsymbol{Q}$ in the Brillouin zone [see Fig. 1(c)]. Here the Pauli matrices $\boldsymbol{\sigma} = (\sigma_x, \sigma_y, \sigma_z)$ refer to the real spin degree of freedom of electrons. They may also refer to pseudospin degree of freedom, which will be discussed later.

We assume that the interaction between the 3D itinerant Weyl fermions and a magnetic impurity $\boldsymbol{S}_i$ located

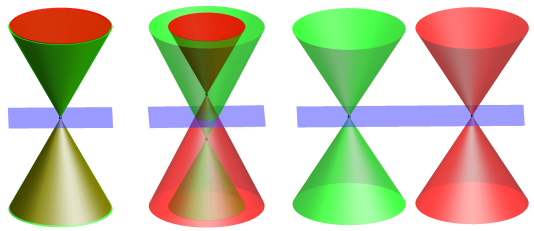

FIG. 1. (Color online) Low energy spectra for Dirac SMs (a), noncentrosymmetric Weyl SMs (b), and Weyl SMs without TRS (c), respectively. The color of cone indicates the chirality of Weyl nodes, while the blue plane is the Fermi level $\varepsilon_F = 0$.

at $\boldsymbol{R}_i$ can be expressed as the standard s-d interaction Hamiltonian $H_I = (J\tau_0 + \lambda\tau_x)\boldsymbol{S}_i \cdot \boldsymbol{\sigma}\delta(\boldsymbol{r} - \boldsymbol{R}_i)$, where J and λ refer to the strength of the s-d exchange interaction in the intranode process and the internode process, respectively. The identity matrix τ_0 and Pauli matrix τ_x act on the chirality space.

According to the second order perturbation theory [25], at zero temperature the RKKY interaction between two magnetic impurities mediated by Weyl fermions is given by $H_{\rm RKKY} = -\frac{1}{\pi}{\rm Im}\int_{-\infty}^{\varepsilon_F} d\varepsilon\, {\rm Tr}[(J\tau_0 + \lambda\tau_x)\boldsymbol{S}_1 \cdot \boldsymbol{\sigma}\mathcal{G}(\boldsymbol{R};\varepsilon)(J\tau_0 + \lambda\tau_x)\boldsymbol{S}_2 \cdot \boldsymbol{\sigma}\mathcal{G}(-\boldsymbol{R};\varepsilon)]$ with $\boldsymbol{R} = \boldsymbol{R}_2 - \boldsymbol{R}_1$, where ε_F is the Fermi energy and Tr means a trace over the spin and pseudospin degree of freedom of itinerant Weyl fermion. The Green function in the energy-coordinate representation is given as $\mathcal{G}(\boldsymbol{R};\varepsilon) = G_+(\boldsymbol{R};\varepsilon) \oplus G_-(\boldsymbol{R};\varepsilon)$. After some algebra, we find the RKKY interaction [26]

$$H_{\rm RKKY} = \sum_{\alpha,\beta,\chi,\chi'} \left[J^2\delta_{\chi\chi'} + \lambda^2(1-\delta_{\chi\chi'})\right] S_1^\alpha S_2^\beta \times {\rm Im}\left[-\frac{1}{\pi}\int_{-\infty}^{\varepsilon_F} d\varepsilon {\rm Tr}[\sigma_\alpha G_\chi(\boldsymbol{R};\varepsilon)\sigma_\beta G_{\chi'}(-\boldsymbol{R};\varepsilon)]\right] , \quad (2)$$

which includes contributions from both the intranode process and the internode process.

We now apply the above formalism to study the RKKY interaction in Dirac and Weyl SMs. We note that close to the Weyl nodes, the effective Hamiltonian is proportional to $\boldsymbol{k}\cdot\boldsymbol{\sigma}$, which can be viewed as the 3D counterpart of graphene in real spin space. It is in contrast with the surface state of 3D topological insulators (TIs) [27–29], in which spin and velocity are perpendicular to each other. As we show below, this kind of hedgehog spin texture around Weyl nodes (spin is aligned with momentum) can have significant effects on the magnetism of magnetic impurities.

Let us first consider the isotropic Dirac SMs, described by $H_{\rm D}(\boldsymbol{k}) = \chi v_F \boldsymbol{k}\cdot\boldsymbol{\sigma}$ with the energy dispersion $\varepsilon_k = \pm v_F k$. The effect of anisotropic energy dispersion will be discussed later. The Green function corresponding to $H_{\rm D}(\boldsymbol{k})$ in momentum space takes the form $G_\chi^{-1}(\boldsymbol{k};\varepsilon) = (\varepsilon + i\eta)\sigma_0 - H_D(\boldsymbol{k})$, where η is a positive infinitesimal. $G_\chi(\pm\boldsymbol{R};\varepsilon)$ can be obtained from $G_\chi(\boldsymbol{k};\varepsilon)$ through integrating over the momentum near the Weyl node χ, $G_\chi(\pm\boldsymbol{R};\varepsilon) = \int \frac{d^3\boldsymbol{k}}{(2\pi)^3} G_\chi(\boldsymbol{k};\varepsilon)\exp(\pm i\boldsymbol{k}\cdot\boldsymbol{R})$. Carrying out the integration over $\boldsymbol{k}$ leads to (more details are presented in the Supplemental Material [30]) $G_\chi(\pm\boldsymbol{R};\varepsilon) = \sigma_0 G_0(R;\varepsilon) \pm \chi\sigma_j G_R(R;\varepsilon)$, where the Green functions are defined as $G_0(R;\varepsilon) = \frac{-\varepsilon}{4\pi v_F^2 R}\exp[i\xi_\varepsilon]$ and $G_R(R;\varepsilon) = \frac{-i}{4\pi v_F R^2}(1 - i\xi_\varepsilon)\exp[i\xi_\varepsilon]$, with the dimensionless parameter $\xi_\varepsilon = \varepsilon R/v_F$. In the above calculation, we take $\boldsymbol{R}$ to be aligned to the j-axis, i.e., $\boldsymbol{R} = R\boldsymbol{e}_j$.

After lengthy but straightforward calculations, we obtain the RKKY interaction for the Dirac SMs (the detailed calculation can be found in the Supplemental Material [30])

$$H^{\rm D}_{\rm RKKY} = F^{\rm D}_{\rm H}(R,\xi_F)\boldsymbol{S}_1\cdot\boldsymbol{S}_2 + F^{\rm D}_{\rm Ising}(R,\xi_F)S_1^jS_2^j , \quad (3)$$

where the range functions for the Heisenberg and Ising terms are given by

$$F^{\rm D}_{\rm H}(R,\xi_F) = -\left\{J^2[(3-2\xi_F^2)\cos(2\xi_F) + 4\xi_F\sin(2\xi_F)] - 2\lambda^2[\cos(2\xi_F) + \xi_F\sin(2\xi_F)]\right\}/8\pi^3 v_F R^5 \quad (4)$$

$$F^{\rm D}_{\rm Ising}(R,\xi_F) = -(J^2-\lambda^2)\left[(2\xi_F^2-5)\cos(2\xi_F) - 6\xi_F\sin(2\xi_F)\right]/8\pi^3 v_F R^5 , \quad (5)$$

with $\xi_F = \varepsilon_F R/v_F$. Here the superscript D stands for Dirac SMs. One can clearly see that if $J^2 = \lambda^2$, the contribution to the Ising term from the internode process cancels that from the intranode process exactly, i.e., $F^{\rm D}_{\rm Ising} = 0$. This cancellation is due to the restoration of the spin rotation symmetry by the internode process.

At long range ($\xi_F \gg 1$) and for finite ε_F, the RKKY interaction reduces to a simple form

$$H^{\rm D}_{\rm RKKY} \approx \frac{J^2\varepsilon_F^2\cos(2\xi_F)}{4\pi^3 v_F^3 R^3}\boldsymbol{S}_1\cdot\boldsymbol{S}_2 , \quad (6)$$

which reflects the long-range and oscillatory nature of the RKKY interaction. The ferromagnetism (FM) or antiferromagnetism (AFM) of magnetic impurities depends on both the concentration of impurities and the carrier density of Dirac fermions through R and ε_F, respectively.

Interestingly, for the intrinsic case ($\varepsilon_F = 0$), the RKKY interaction becomes nonoscillatory

$$H^{\rm D}_{\rm RKKY} = \frac{-(3J^2-2\lambda^2)}{8\pi^3 v_F R^5}\boldsymbol{S}_1\cdot\boldsymbol{S}_2 . \quad (7)$$

We can see that if $J^2 = \lambda^2$, the exchange coupling is always ferromagnetic. For sufficiently large impurity density, this will lead to a spontaneous magnetization, which then drives Dirac SMs into Weyl SMs with broken TRS. Consequently, a nonzero anomalous Hall conductivity proportional to the separation of the two Weyl nodes

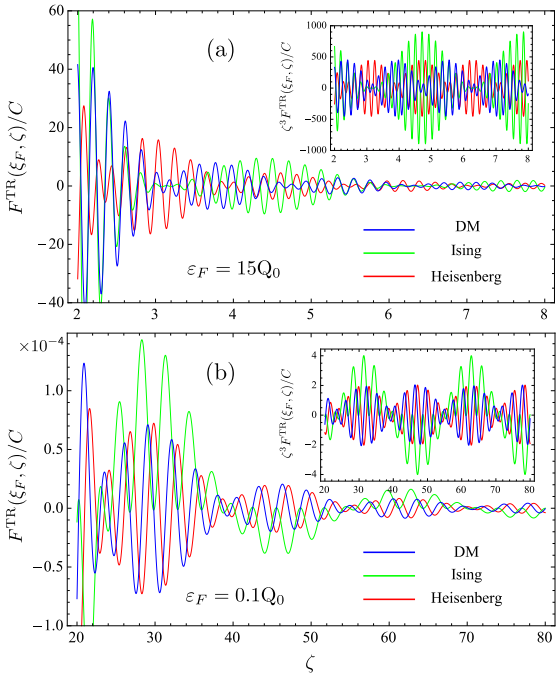

FIG. 2. (Color online) The exact range functions of RKKY interaction of the noncentrosymmetric Weyl SMs (F^{TR}/C) as a function of the reduced parameter ζ at the Fermi energy $\varepsilon_F =$ 15 Q_0 (a) and $\varepsilon_F = 0.1$ Q_0 (b), with $C = -J^2\mathrm{Q}_0^5/(2\pi v_F^2)^3$. The inset in each panel for $\zeta^3 F^{TR}/C$ shows an evident beating feature for each term in this RKKY interaction.

in momentum space will appear [31]. The ferromagnetic transition temperature T_c depends on the specifics of both magnetic impurities and host materials, which need detailed first-principles studies [32]. It is clear that its spatial dependence as $1/R^5$ differs from $1/R^3$ for the intrinsic graphene [33].

Next we consider noncentrosymmetric Weyl SMs, in which the two Weyl nodes with opposite chirality have different energies ($\mathrm{Q}_0 \neq 0$). For a given carrier density, the magnitudes of Fermi wave vectors of these two Weyl nodes are distinct, therefore $\xi_F^+ \neq \xi_F^-$ with $\xi_F^\chi = (\varepsilon_F - \chi\mathrm{Q}_0)R/v_F$. Following the same procedure, we obtain the RKKY interaction for the noncentrosymmetric Weyl SMs

$$H_{\mathrm{RKKY}}^{\mathrm{TR}} = F_{\mathrm{H}}^{\mathrm{TR}}(\xi_F,\zeta)\boldsymbol{S}_1\cdot\boldsymbol{S}_2 + F_{\mathrm{Ising}}^{\mathrm{TR}}(\xi_F,\zeta) \times S_1^j S_2^j + F_{\mathrm{DM}}^{\mathrm{TR}}(\xi_F,\zeta)(\boldsymbol{S}_1\times\boldsymbol{S}_2)_j\ , \quad (8)$$

with $\zeta = \mathrm{Q}_0 R/v_F$ and the jth-component of the spin S^j is along the direction connecting the two impurities. Here the superscript TR stands for the TRS invariant Weyl SMs. We can see that the RKKY interaction consists of three terms, namely, a Heisenberg term, an Ising term and a Dzyaloshinsky-Moriya (DM) term [34]. This is similar to the surface state of TIs [28]. The specific expressions of these range functions ($F_{\mathrm{H}}^{\mathrm{TR}}, F_{\mathrm{Ising}}^{\mathrm{TR}}, F_{\mathrm{DM}}^{\mathrm{TR}}$) are given in the Supplemental Material [30].

Figure 2 shows the range functions to two sets of parameters. As we can see, these range functions display a damped oscillatory behavior with increasing distance R, with each term dominating in different regime of the parameters ε_F and R. In addition, these range functions oscillate with two distinct periods and form a beating pattern. The beating feature, originated from the two unequal Fermi wavevectors, manifests itself by multiplying each of range functions in Eq. (8) by ζ^3 as shown in the insets of Figs. 2(a) and 2(b). The measurement of beating period can be used to determine the energy difference Q_0 [35]. This beating structure does not occur in the typical surface state of TIs where there is only one Fermi circle [27–29].

The DM term is essential for realizing spiral spin states and skyrmions, and also has potential applications in spintronics. It may also provide some hint to understand the recent experimental observation of the TRS-breaking Weyl metal in $YbMnBi_2$ [23]. In this material, although there is a global inversion symmetry, in each layer the inversion symmetry is broken, which could give rise to a nonvanishing DM term. The combination of the DM interaction and the AFM order of Mn can cause a canted AFM order with a nonvanishing net magnetization observed in the experiment [23].

Finally, we discuss TRS-breaking Weyl SMs, in which the Weyl nodes with opposite chirality reside at different $\boldsymbol{k}$-points in momentum space $\pm\boldsymbol{Q}$. We further assume the inversion symmetry remains intact, thus the DM term does not appear. We take into account the effect of the separation of Weyl nodes in the internode process. The corresponding RKKY interaction can be obtained from that of Dirac SMs in Eqs. (4) and (5) by replacing λ^2 with $\lambda^2\cos(2\boldsymbol{Q}\cdot\boldsymbol{R})$. It can be seen that the internode process gives rise to an oscillating term proportional to $\sim\cos(2\boldsymbol{Q}\cdot\boldsymbol{R})$, which is absent in the typical surface state of TIs [27, 28]. Because of the long-range and oscillatory nature of the RKKY interaction, for a large momentum separation $2\boldsymbol{Q}$, the part from the internode process will vanish after averaging over position and thus does not contribute to the net magnetization. Therefore, the intranode process dominates the RKKY interaction in this case. At long distance, we have the approximate RKKY interaction

$$H_{\mathrm{RKKY}}^{\mathrm{I}} \approx \frac{J^2\varepsilon_F^2\cos(2\xi_F)}{4\pi^3 v_F^3 R^3}(\boldsymbol{S}_1\cdot\boldsymbol{S}_2 - S_1^j S_2^j)\ , \quad (9)$$

where the superscript I refers to the centrosymmetric Weyl SMs. Since the asymptotic range functions for the Heisenberg and Ising terms exhibit the same oscillatory behavior but with a phase differing by π, the Ising term always cancels the j-th component of the Heisenberg term, leading to the XY-like spin model for $j = z$. On the other hand, for the intrinsic case the RKKY interaction becomes

$$H_{\mathrm{RKKY}}^{\mathrm{I}} = \frac{-J^2}{8\pi^3 v_F R^5}(3\boldsymbol{S}_1\cdot\boldsymbol{S}_2 - 5S_1^j S_2^j)\ , \quad (10)$$

which could realize various spin models, such as the XXZ-like spin model for $j = z$. The resulting spin configurations of impurities (XY- and XXZ-like spin models) can be accessed by a variety of experimental techniques, such as neutron scattering technique.

In reality, almost all experimental realizations of Weyl or Dirac SMs (and theoretically conjectured systems, such as [31, 36–38]) possess a strongly anisotropic single-particle dispersion. Here we consider the effect of anisotropy on the RKKY interaction. The effective Hamiltonian for fermions near the anisotropic Weyl node χ takes the form $\tilde{H}_0 = \chi(v_x\tilde{k}_x\sigma_x + v_y\tilde{k}_y\sigma_y + v_z\tilde{k}_z\sigma_z)$, where the Fermi velocities v_α in different direction are different, $|v_x| \neq |v_y| \neq |v_z|$. To simplify our discussion, we set $v_j > 0$ with $j = x, y, z$. The corresponding energy spectrum is given as $\varepsilon_{\tilde{k}} = \pm(v_x^2\tilde{k}_x^2 + v_y^2\tilde{k}_y^2 + v_z^2\tilde{k}_z^2)^{1/2}$. It is instructive to make the following transformation as $(v_i\tilde{Q}_i, v_i\tilde{k}_i, v_F\tilde{R}_i) \equiv (v_FQ_i, v_Fk_i, v_iR_i)$, such that we relate the Green function of an anisotropic Weyl node in the energy-coordinate representation to that of an isotropic one as $\tilde{G}_\chi(\pm\tilde{\boldsymbol{R}};\varepsilon) = \lambda_A G_\chi(\pm\boldsymbol{R};\varepsilon)$, with $\lambda_A = v_F^3/(v_xv_yv_z)$. We note that the above transformation converts a Fermi elliptic sphere into a Fermi sphere but preserves the volume of Fermi sphere. This allows us to connect the RKKY interaction of anisotropic Dirac SMs to the counterpart of the isotropic ones

$$\tilde{H}_{\rm RKKY}(\tilde{R}) = \lambda_A^2 H_{\rm RKKY}(v_F\tilde{R}/v_i)\ , \qquad (11)$$

which implies that the anisotropy of Dirac or Weyl nodes must lead to an anisotropic RKKY interaction. It is clear that for $v_x = v_y = v_z$ ($\lambda_A = 1$), the above expression in Eq. (11) can reduce to that of the isotropic one.

Before drawing conclusions, we briefly discuss the pseudospin case, in which the Pauli matrices in Eq. (1) may refer to pseudospin degree of freedom such as orbital index. This pseudospin case is similar to graphene. In the absence of the spin-momentum locking, the RKKY interaction only contains the conventional Heisenberg term [39]. Hence, the RKKY interaction directly associates with the Fourier transform of the static density-density response function [40]. We leave all the specific expressions of RKKY interaction to the Supplemental Material [30]. It should be emphasized that the RKKY interaction in this intrinsic Dirac SMs is also a nonoscillatory Heisenberg term $H_{\rm RKKY} = \frac{(2J^2-3\lambda^2)}{4\pi^3 v_F R^5}\boldsymbol{S}_1\cdot\boldsymbol{S}_2$, which allows the spontaneous magnetization of magnetic impurities for $|\lambda| > (2/3)^{1/2}|J|$. Compared with Eq. (7), the factor of 2 comes from the degeneracy of real spin degree of freedom.

In summary, we have studied the RKKY interaction between magnetic impurities in Dirac and Weyl SMs. We found that it is possible to realize a spontaneous magnetization in these systems. The RKKY interaction in general contains the Heisenberg, Ising, and DM terms, which can give rise to rich spin textures of the impurities. These findings provide an alternative scheme to engineer topological SMs and pave the way for the application of Dirac and Weyl SMs for spintronics.

We are grateful to Ran Cheng and Shengyuan Yang for many valuable discussions and comments. This work is supported by AFOSR (No. FA9550-14-1-0277), NSF (No. EFRI-1433496), Natural Science Foundation of Sichuan Educational Committee (Grant No. 13ZB0157) and Sichuan Normal University (Grant No. 15YB001).

Note added.–After the submission of this manuscript, a related paper appeared, in which some results on the anisotropic Weyl SMs has also been obtained in [41]. Recently, the Kondo effect of a single magnetic impurity in the Weyl SMs has also been discussed in [42].

* jianhuizhou1@gmail.com
† dixiao@cmu.edu

[1] S. M. Young, S. Zaheer, J. C. Y. Teo, C. L. Kane, E. J. Mele, and A. M. Rappe, Phys. Rev. Lett. **108**, 140405 (2012).
[2] X. Wan, A. M. Turner, A. Vishwanath, and S. Y. Savrasov, Phys. Rev. B **83**, 205101 (2011).
[3] G. E. Volovik, *The Universe in a Helium Droplet* (Clarendon, Oxford, UK, 2003).
[4] D. Xiao, M.-C. Chang, and Q. Niu, Rev. Mod. Phys. **82**, 1959 (2010).
[5] H. Wei, S.-P. Chao, and V. Aji, Phys. Rev. Lett. **109**, 196403 (2012).
[6] G. Y. Cho, J. H. Bardarson, Y.-M. Lu, and J. E. Moore, Phys. Rev. B **86**, 214514 (2012); S. A. Yang, H. Pan, and F. Zhang, Phys. Rev. Lett. **113**, 046401 (2014).
[7] S.-Y. Xu, C. Liu, S. K. Kushwaha, R. Sankar, J. W. Krizan, I. Belopolski, M. Neupane, G. Bian, N. Alidoust, T.-R. Chang, H.-T. Jeng, C.-Y. Huang, W.-F. Tsai, H. Lin, P. P. Shibayev, F.-C. Chou, R. J. Cava, and M. Z. Hasan, Science **347**, 294 (2015).
[8] X.-Q. Sun, S.-C. Zhang, and Z. Wang, Phys. Rev. Lett. **115**, 076802 (2015).
[9] P. Hosur and X. Qi, C. R. Phys. **14**, 857 (2013); A. A. Burkov, J. Phys.: Condens. Matter **27**, 113201 (2015), and references therein.
[10] S. T. Ramamurthy and T. L. Hughes, Phys. Rev. B **92**, 085105 (2015).
[11] A. A. Zyuzin and A. A. Burkov, Phys. Rev. B **86**, 115133 (2012); J.-H. Zhou, H. Jiang, Q. Niu, and J.-R. Shi, Chin. Phys. Lett. **30**, 027101 (2013); M. M. Vazifeh and M. Franz, Phys. Rev. Lett. **111**, 027201 (2013); S. A. Parameswaran, T. Grover, D. A. Abanin, D. A. Pesin, and A. Vishwanath, Phys. Rev. X **4**, 031035 (2014); M.-C. Chang and M.-F. Yang, Phys. Rev. B **91**, 115203 (2015); S. Zhong, J. Orenstein, and J. E. Moore, Phys. Rev. Lett. **115**, 117403 (2015).
[12] D. T. Son and B. Z. Spivak, Phys. Rev. B **88**, 104412 (2013); A. A. Burkov, Phys. Rev. Lett. **113**, 247203 (2014); H.-Z. Lu, S.-B. Zhang, and S.-Q. Shen, Phys. Rev. B **92**, 045203 (2015).
[13] Q. Jiang, H. Jiang, H. Liu, Q. Sun, and X. Xie, arXiv:1501.06535 (2015); S. A. Yang, H. Pan, F. Zhang,

arXiv:1504.00732 (2015).
[14] M. Brahlek, N. Bansal, N. Koirala, S.-Y. Xu, M. Neupane, C. Liu, M. Z. Hasan, and S. Oh, Phys. Rev. Lett. **109**, 186403 (2012).
[15] Z. K. Liu, B. Zhou, Y. Zhang, Z. J. Wang, H. M. Weng, D. Prabhakaran, S.-K. Mo, Z. X. Shen, Z. Fang, X. Dai, Z. Hussain, and Y. L. Chen, Science **343**, 864 (2014).
[16] S. Borisenko, Q. Gibson, D. Evtushinsky, V. Zabolotnyy, B. Büchner, and R. J. Cava, Phys. Rev. Lett. **113**, 027603 (2014).
[17] H. Weng, C. Fang, Z. Fang, B. A. Bernevig, and X. Dai, Phys. Rev. X **5**, 011029 (2015).
[18] S.-Y. Xu, I. Belopolski, N. Alidoust, M. Neupane, C. Zhang, R. Sankar, S.-M. Huang, C.-C. Lee, G. Chang, BaoKai Wang, G. Bian, H. Zheng, D. S. Sanchez, F. Chou, H. Lin, S. Jia, M. Z. Hasan, arXiv:1502.03807 (2015).
[19] B. Q. Lv, H. M. Weng, B. B. Fu, X. P. Wang, H. Miao, J. Ma, P. Richard, X. C. Huang, L. X. Zhao, G. F. Chen, Z. Fang, X. Dai, T. Qian, and H. Ding, Phys. Rev. X **5**, 031013 (2015).
[20] S.-Y. Xu, N. Alidoust, I. Belopolski, C. Zhang, G. Bian, T.-R. Chang, H. Zheng, V. Strokov, D. S. Sanchez, G. Chang, Z. Yuan, D. Mou, Y. Wu, L. Huang, C.-C. Lee, S.-M. Huang, B. Wang, A. Bansil, H.-T. Jeng, T. Neupert, A. Kaminski, H. Lin, S. Jia, M. Z. Hasan, arXiv:1504.01350 (2015).
[21] C. Shekhar, A. K. Nayak, Y. Sun, M. Schmidt, M. Nicklas, I. Leermakers, U. Zeitler, Y. Skourski, J. Wosnitza, Z. Liu, Y. Chen, W. Schnelle, H. Borrmann, Y. Grin, C. Felser, and B. Yan, Nat. Phys **11**, 645 (2015).
[22] N. Xu, H. M. Weng, B. Q. Lv, C. Matt, J. Park, F. Bisti, V. N. Strocov, D. gawryluk, E. Pomjakushina, K. Conder, N. C. Plumb, M. Radovic, G. Auts, O. V. Yazyev, Z. Fang, X. Dai, G. Aeppli, T. Qian, J. Mesot, H. Ding, M. Shi, arXiv:1507.03983 (2015).
[23] S. Borisenko, D. Evtushinsky, Q. Gibson, A. Yaresko, T. Kim, M. N. Ali, B. Buechner, M. Hoesch, R. J. Cava, arXiv:1507.04847.
[24] C.-Z. Chang, J. Zhang, X. Feng, J. Shen, Z. Zhang, M. Guo, K. Li, Y. Ou, P. Wei, L.-L. Wang, Z.-Q. Ji, Y. Feng, S. Ji, X. Chen, J. Jia, X. Dai, Z. Fang, S.-C. Zhang, K. He, Y. Wang, L. Lu, X.-C. Ma, and Q.-K. Xue, Science **340**, 167 (2013); X. Kou, S.-T. Guo, Y. Fan, L. Pan, M. Lang, Y. Jiang, Q. Shao, T. Nie, K. Murata, J. Tang, Y. Wang, L. He, T.-K. Lee, W.-L. Lee, and K. L. Wang, Phys. Rev. Lett. **113**, 137201 (2014); J. G. Checkelsky, R. Yoshimi, A. Tsukazaki, K. S. Takahashi, Y. Kozuka, J. Falson, M. Kawasaki, and Y. Tokura, Nat. Phys. **10**, 731 (2014); C.-Z. Chang, W. Zhao, D. Y. Kim, H. Zhang, B. A. Assaf, D. Heiman, S.-C. Zhang, C. Liu, M. H. W. Chan, and J. S. Moodera, Nature Materials **14**, 473(2015).
[25] G. D. Mahan, *Many-Particle Physics*, 3rd ed. (Springer, New York, 2007).
[26] For realistic systems with multiple pairs of Weyl nodes, the full RKKY interaction contains the contributions from both the intra-pair and the inter-pair processes. Since the momentum spacing between different pairs is usually large such that the contributions from inter-pair processes oscillates fast. Thus, the contributions from the intra-pair processes will dominate. The total RKKY interaction becomes a direct summation of those of different pairs. In our manuscript, we focus on this case. In fact, these contributions from the inter-pair processes can also be calculated in a similar mean.
[27] Q. Liu, C.-X. Liu, C. Xu, X.-L. Qi, and S.-C. Zhang, Phys. Rev. Lett. **102**, 156603 (2009).
[28] J.-J. Zhu, D.-X. Yao, S.-C. Zhang, and K. Chang, Phys. Rev. Lett. **106**, 097201 (2011).
[29] R. R. Biswas and A. V. Balatsky, Phys. Rev. B **81**, 233405 (2010).
[30] See Supplemental Material for calculation of the Green function in the energy-coordinate representation, derivation of the expressions of the range functions in the RKKY interaction for both the Dirac and Weyl SMs, and relation of the RKKY interaction between the isotropic Dirac or Weyl SMs and the anisotropic ones.
[31] K.-Y. Yang, Y.-M. Lu, and Y. Ran, Phys. Rev. B **84**, 075129 (2011).
[32] T. Jungwirth, J. Sinova, J. Mašek, J. Kučera, and A. H. MacDonald, Rev. Mod. Phys. **78**, 809 (2006).
[33] E. Kogan, Phys. Rev. B **84**, 115119 (2011).
[34] I. Dzyaloshinsky, J. Phys. Chem. Solids **4**, 241 (1958); T. Moriya, Phys. Rev. **120**, 91 (1960).
[35] The length of beating for each term is roughly determined by Sine or Cosine function of 2ζ for the Fermi energy $\varepsilon_F = 15\mathrm{Q}_0$ and of $2\xi_F$ for $\varepsilon_F = 0.1\mathrm{Q}_0$. The behavior of the beating can be gained from the asymptotic expressions [30].
[36] G. Xu, H. Weng, Z. Wang, X. Dai, and Z. Fang, Phys. Rev. Lett. **107**, 186806 (2011).
[37] Z. Wang, Y. Sun, X.-Q. Chen, C. Franchini, G. Xu, H. Weng, X. Dai, and Z. Fang, Phys. Rev. B **85**, 195320 (2012).
[38] Z. Wang, H. Weng, Q. Wu, X. Dai, and Z. Fang, Phys. Rev. B **88**, 125427 (2013).
[39] M. A. Ruderman and C. Kittel, Phys. Rev. **96**, 99 (1954); T. Kasuya, Prog. Theor. Phys. **16**, 45 (1956); K. Yosida, Phys. Rev. **106**, 893 (1957).
[40] J. Zhou, H.-R. Chang, and D. Xiao, Phys. Rev. B **91**, 035114 (2015).
[41] Mir Vahid Hosseini, M. Askari, arXiv:1510.03020 (2015).
[42] J.-H. Sun, D.-H. Xu, F.-C. Zhang, Y. Zhou, arXiv:1509.05180 (2015).